A Multi-Axis FBG-Based Tactile Sensor for Gripping in Space

Samuel Frishman*[1], Julia Di*[1], Zulekha Karachiwalla[2], Richard J. Black[3], Kian Moslehi[3], Trey Smith[4], Brian Coltin[4], Bijan Moslehi[3], Mark R. Cutkosky[1]

***Abstract*— Tactile sensing offers the ability to improve end-effector control and grasp quality, especially for floating platforms, which may not always approach a target with accurate alignment. Furthermore, the development of robust and accurate tactile sensors remains a challenge for harsh environments like space. We present a sensing approach intended, for example, to be mounted on a gripper attached to Astrobee free-flyers in the International Space Station (ISS). The gripper uses a single optical fiber with Bragg grating (FBG) sensors to measure normal and shear strains in the gripping pads. In comparison to conventional wired solutions, the encapsulated optical fiber is robust and its signals are immune to electromagnetic interference. Sampling is possible at over 1 kHz to detect dynamic events. We mount the sensor on a two-phalange gripper with independent control of the distal and proximal phalanges, allowing for grip readjustment based on sensing data. We perform experiments that demonstrate capabilities enabled by the sensing technology and gripper design, motivated by Astrobee tasks. Specifically, we explore gripping corners, detecting misaligned grasps, and optimizing the contact area in pinch grasps.**

I. INTRODUCTION

Space exploration presents vast opportunities for robotic systems as well as unique challenges. Radiation, electromagnetic interference (EMI), and extreme temperatures limit technologies and devices used for space applications. Nevertheless, robots and automation are central to enabling exploration of more distant and dangerous locations. The importance of tactile sensing in robotic systems designed for unstructured and unknown environments is increasingly recognized [REF]. Prevalent sensing modalities, capacitive and resistive, however, are prone to noise and often require near-sensor processing. We introduce an optical-based multi-axis tactile sensor for robotic grippers in space (Fig. 1). The initial version is created for the Asbrobee Free-Flyer on the ISS [1], with the underlying design conducive to future extra-vehicular applications (Robonaut 2?).

Among the many technologies considered for tactile sensing, optical sensors provide a number of advantages including EMI resistance, durability, resistance to corrosion, etc. [2]. In particular, fiber optic sensors using Fiber Bragg Gratings (FBGs), can withstand extreme temperatures (cryogenic to 1000°C) and radiation [REF]. Moreover, FBGs exhibit excellent signal-to-noise ratio (SNR) and sensitivity to very small strains. They can also route over long distances with negligible loss.

Leveraging fiber technology, we introduce an novel sensing pad with towers embedded inside a urethane elastomer. The pad is composed of four isolated sensing towers, each with four FBGs. Additionally, the pad includes a strain isolated FBG for temperature compensation. In total, the sensor consists of 17 FBGs, all routed on a single fiber. The sensor is applied to a custom, two finger two phalange gripper. The design is inspired by the Asrobee perching gripper [1] with increased functionality to leverage the tactile sensor. Specifically, the gripper provides two controllable degrees-of-freedom with independent actuation of the distal and proximal phalanges. The distal phalange includes ability to extend backward to achieve planer contact during pinch or corner grasps. In the following sections we describe the sensor and gripper designs and report on experiments conducted to characterize the sensor and demonstrate its performance. Specifically, we use the sensor to make grasp adjustments and modulate grasp force.

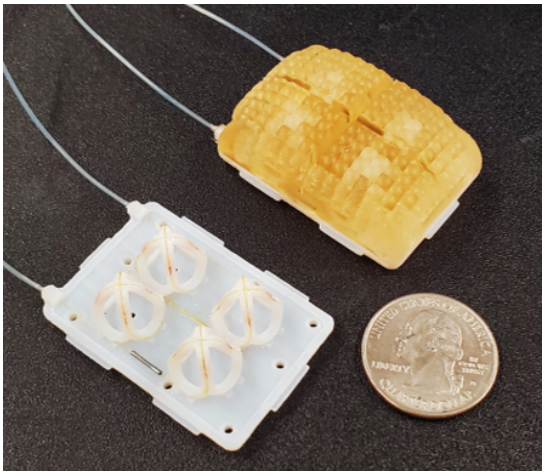

Fig. 1. An FBG-based, multi-axis sensing pad. Tower structures, embedded with FBGs, provide three-axis force information at each structure location. An additional FBG is isolated inside a metal sleeve and provides temperature compensation. The sensing unit is encapsulated inside a urethane elastomer, which serves as the gripping surface. Grooves in the cover decouple signal between the towers.

A. Related Work

FBGs provide strain information through changes in wavelength. Their durability is leveraged in a wide range of applications including oil and gas [3], wind energy [4], and

*These authors contributed equally

[1]Stanford University, Department of Mechanical Engineering, Stanford, California 94305

[2]University of Maryland, Department of Computer Engineering, Baltimore, Maryland 21250

[3] Intelligent Fiber Optic Systems Corporation, San Jose, California 95134

[4] NASA Ames, Mountain View, California 94035

medical devices [5]. To date, FBG based tactile sensors have been largely limited to a single-axis sensing (e.g. pressure) [6]–[12]. Embodiments capable of multi-axis sensing have been comparatively large (e.g. designed for use a multi-axis force/torque sensor) [13], [14] or embedded directly into gripper fingers [15]–[17].

Opportunities remain to use FBG technology for sensing spatially distributed, multi-axis forces on gripper phalanges. Specifically, understanding grasp contact area and phalange-object alignment can improve grasp quality. The importance of these parameters has been well noted [REFS Aaron Dollar], in particular for underactuated grippers. Typically, underactuated designs exhibit a trade-off between pulleys and joint stiffness values to optimize gripper performance. Ciocarlie et al. [18] finely tune spring stiffnesses to maintain a parallel constraint on the distal phalanges, unless impact is made proximaly, and enable planer contact in pinch grasps. Linkage mechanisms have also been explored to achieve similar grasp trajectories [REF]. While robust designs, these examples are limited to specific grasp trajectories and forces. Utilizing the FBG sensing pad enables a wider range of grasps with adjustment of contact area, modulation of forces, and understanding of off-axis alignment (e.g. with a hand rail or cylindrical tool).

II. Sensor Design

Sensor design is constrained by optical fiber requirements. Specifically, routing must satisfy set minimum bend radii and accommodate pre-determined FBG lengths. For 125μ and 80μ fiber, bend radii should not fall below 6mm and 4mm, respectively, and typical FBG lengths are either four or two mm. For a sensing pad, particularly one designed for a small gripper, our goal is to create the smallest sensing tower possible while observing these constraints. Moreover, to achieve multi-axis sensing, we include multiple FBGs per tower. The resulting tower structure is illustrated in Fig 2. The fiber routes through four pillars connected by rounded sections of 4mm radius. The pillars are 4mm in length, accommodating a 2mm FBG with 1mm buffer on either end for error in placement. We note that it is critical for FBGs to be placed on a straight section to avoid double peaks in signal [6]. Pillar angle, θ_p, determines structure sensitivity to normal vs. shear forces. For this prototype, informed by the FEA below, a 70° angle is selected to achieve a desirable balance. These parameters fully define the tower geometry. A groove is included to embed the fiber and additional guide features are added to assist in routing. The groove is of minimum depth to embed the fiber in order to maintain maximum distance from the pillar neutral axis. Towers are tiled to enable spatial sensing of forces and computation of moments. To accommodate a gripper phalange, the sensor is designed slightly longer than it is wide. A single fiber, with custom spacing of FBGs, routes through all four towers of the sensor. An additional FBG is strain isolated inside a metal tube to provide temperature compensation. In total, the fiber has includes 17 FBGs 2. The large number of bends results in significant signal attenuation down the length of the fiber. Additionally, to fit the gripper form factor, towers were designed with a bend radius below the recommended minimum for 125μ fiber. To receive strong signals despite the attenuation, we read the fiber from both ends, using the stronger signal as the given FBG value (Fig. 2B).

The structure is printed on the Stratasys Objet24 and cast inside a urethane elastomer (Smooth-On VytaFlex 20). The urethane cover includes grooves separating each tower to isolate coupling in signal between towers. Fig. 2C presents sample data gathered from all four towers with only one tower under loading. Large strain values are observed by the tower under loading, with minimal signal from adjacent towers.

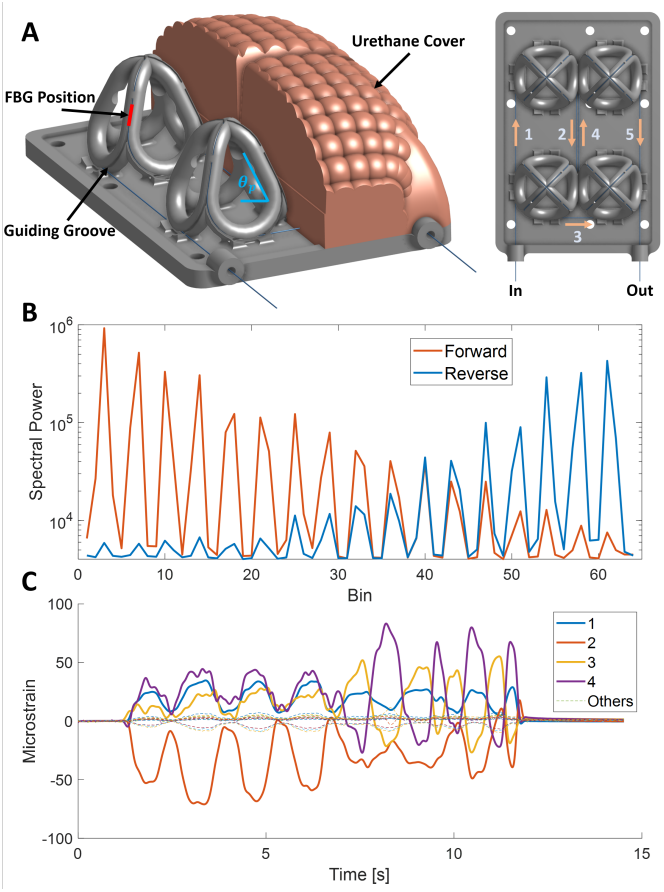

Fig. 2. (A) The sensing structures and urethane cover. Towers include channels to guide the fiber and features to fix the FBG along the pillar straights (red). A single fiber routes through all four towers. (B) The fiber is read from both the forward and reverse directions to minimize attenuation from bending. Seventeen peaks are visible, corresponding to each FBG. The strongest signal for a given FBG is used. (C) Sample data gathered while applying loads on a single taxel. Minimal coupling is visible between towers due to channels in the urethane cover separating the internal structures.

A. FEA

Sensor design is informed by a finite element analysis (FEA). We investigate sensitivity to normal and shear forces and compare tower structures with and without cutout features. The cutouts promote bending in the pillars, which are otherwise largely influenced by axial strain. In a weightless environment, and specifically for Asbrobee tasks, shear

forces are expected to be relatively small compared to normal loads. Accordingly, pillar angle is tuned for increased shear sensitivity. In the FEA, we apply a 1N normal force and 0.33N shear. Results are shown in Fig. 3.

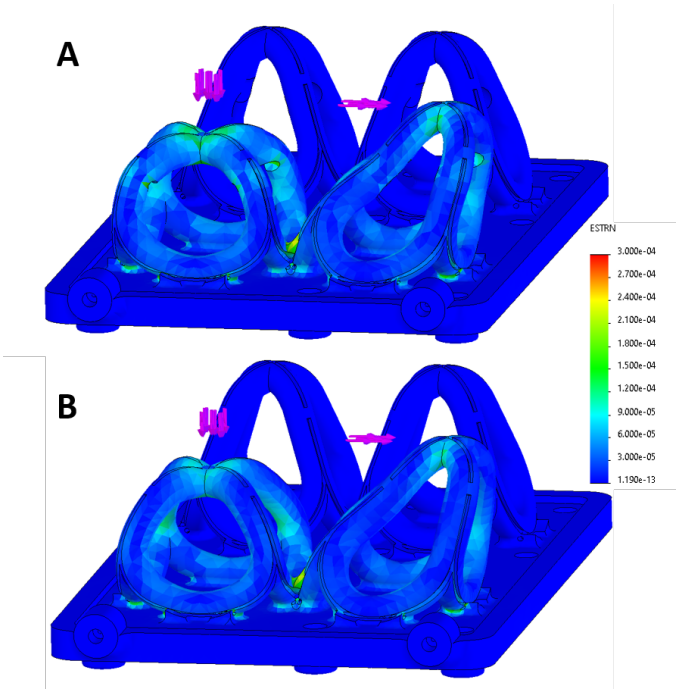

Fig. 3. Finite element analysis. Normal and shear forces are applied to tower structures. (A) The structure includes cutout features in the pillars. (B) Without the cutouts. Significantly more strain is observed at the FBG location in case A. Moreover, tower angle results in a desirable ratio between normal and shear force sensitivity.

III. Gripper Design

A two-phalange two-finger design is selected to resemble the form factor of the current Astrobee gripper [1]. With only one actuated DoF, the existing Asrobee gripper is designed for enveloping grasps with limited ability to perform pinches or meaningfully grasp object corners. We add an additional DoF to provide independent control of the distal and proximal phalanges and enable a range of new grasps. Our design is illustrated in Fig. 4 and includes a "distal backboard" to allow distal hyperextension (backward rotation of the distal phalange from its initial position). The backboard is loaded with an extension spring and pushes against the distal phalange, overpowering the distal torsion spring and forcing the phalange forward. A stopper prevents the backboard from rotating inward beyond the neutral position of the distal phalange. Consequently, this configuration enables the gripper to exhibit a desirable grasp envelope in it's initial configuration, while still enabling planer contact in pinches and corner grasps through hyperexstension of the distal phalange. The motor actuating the proximal phalange must overpower the backboard spring for hyperextension to occur and as such, the spring pre-loaded to minimally exceed the torque from the distal torsion spring.

The gripper body houses two Portescap motors (Part TODO), one for actuating each of the two tendons. Fig. 4 illustrates routing paths to the proximal and distal phalanges. The motors and pulleys are sized to provide near 90N of tension in the cable, providing a XN grasp force in pinch. Moreover, the selected motors are relatively backdrivable (27:1 gear ratio), enabling hyperextension of the distal phalange through backdriving the distal motor. Tendons are anchored to swivel-head screws for ease of tensioning. Stopper features are placed at both the proximal and distal phalanges to limit extension and allow pre-loading the joint torsion springs.

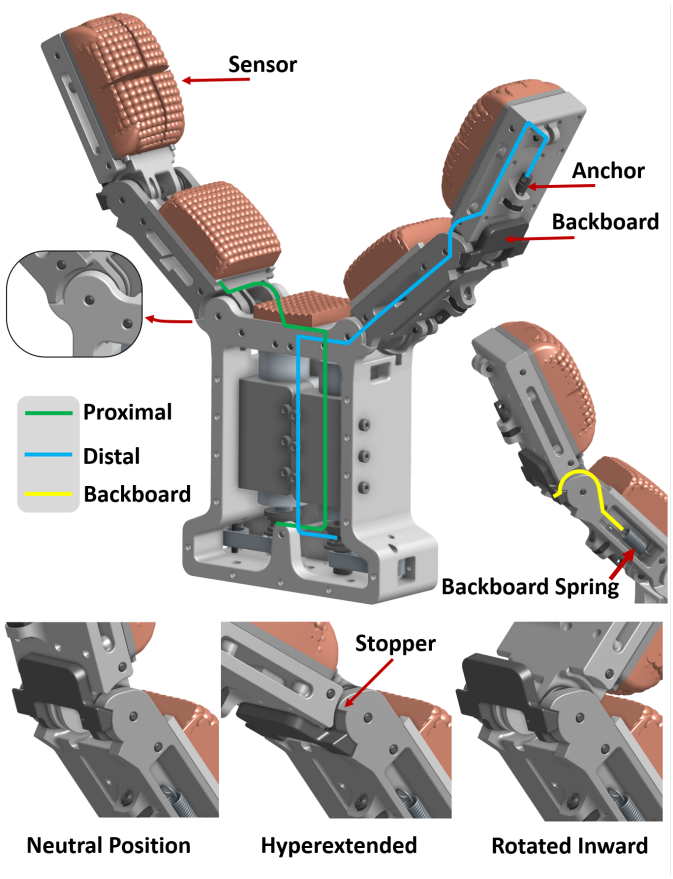

Fig. 4. A custom, two finger gripper with the sensing pad mounted at the distal phalange. Two motors route to independent proximal and distal tendons, providing an underactuated design with two controllable DoF. A backboard feature, loaded by a spring embedded inside the proximal phalange, provides a biasing force inward on the distal phalange and rests against a stopper in the neutral position. The backboard rotates with the distal phalange during hyperextension, further tensioning the backboard spring. During inward rotation, the backboard remains pushed against the stopper.

IV. Experiments

A. Calibration

We calibrate the sensor by mounting the pad on a commercial ATI Gamma F/T load cell and applying randomized forces with a flat, rigid object. Each sensor taxel is calibrated independently and the test set up is shown in the inset of Fig. 5. Raw strain values from the FBGs are collected at 600 Hz.

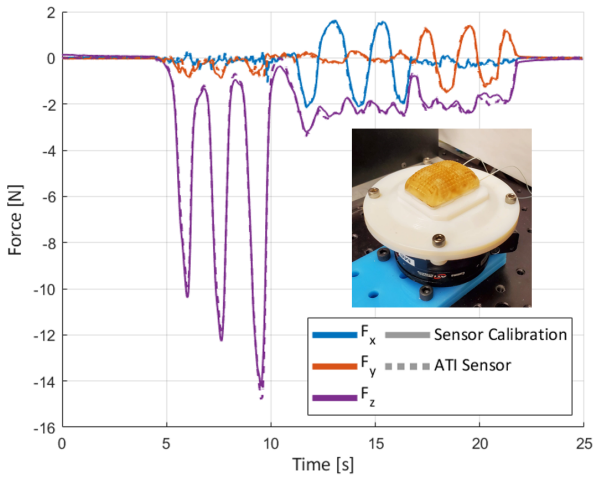

Fig. 5. Sensor calibration of normal and shear forces compared to the ATI, with an R^2 = 0.9956. Inset is picture of testing setup, with the sensor rigidly mounted on top of the ATI. Forces are applied manually to each taxel, which is also transferred to the ATI below.

Because we read the fiber from both the forward and reverse direction in order to mitigate signal attenuation, as shown in Fig. 2b, there is some signal jitter that occurs when switching between the two directions. For a stable signal, we collect three samples and discard two to account for signal jitter, for an overall revisit rate of 100 Hz per fiber direction. The ATI Gamma F/T load cell is also sampled at 100 Hz. We apply low pass filters with a cutoff frequency of 15 Hz on both the sensor and ATI data to reduce any high-frequency noise. The acquisition frequency can be up to 6 kHz, but we collected samples at a lower frequency for less complicated processing downstream.

A second order polynomial fit is done to map the filtered output from a single sensor taxel to the three ATI forces. For the taxel shown in Fig. 5, we achieve an R^2 value of 99.56% on our training data, with a cross-validation R^2 of 97.34% on unseen data, indicating a close fit to the ATI. For all taxels from both sensors, we see calibration R^2 values above 90%, with an average value of 96.17% across taxels on training data.

B. Grasping Evaluation

We conducted preliminary experiments with the sensorized gripper executing different types of grasps, as shown in Fig. 6. These grasping tasks are motivated by real-world tasks that an Astrobee free-flyer might execute on the ISS, such as moving boxes or grabbing tools and supplies. The three experiment tasks we conducted were: detection of misalignment with the object, which is especially a concern for free-flying robots; optimization of contact area for pinch grasps; and novel grasping configurations enabled by sensory feedback, such as gripping the corners of boxes.

Describe experiment tasks...grasping box corner until planer contact achieved and then increasing distal tendon force. Also describe our (maybe novel?) controller where we actuate proximal until planer contact, then proximal does position control to hold that position (based on encoder) while distal increases tension. can get strong corner and pinch grasps using this control algorithm. include box diagram.

Algorithm 1 Hybrid Force-Position Controller

Closing Proximal
while $F_{backTaxels} < Threshold$ **do**
  $error = Threshold - F_{backTaxels}$;
  actuate proximal(pwm∼error);
end
hold proximal position → position control via encoder
Closing Distal
while $F_{frontTaxels} < F_{backTaxels}$ **do**
  $error = F_{frontTaxels} - F_{backTaxels}$;
  actuate distal(pwm∼error)
end

V. Results

Calibration data + experiment data from demo tasks on gripper and figure of it grasping different things (especially box corner and pinch).

With the sensor, we are able to adjust grasps for misalignment.

VI. Discussion

discussion on how to improve sensor... discussion on gripper: need's more control authority, can have bigger motor for proximal since smaller lever arm for distal. control algorithm can be improved with more consideration for shear to try and minimize ejection.

VII. Future Work

There are three directions in which this work could be extended. First, additional testing is needed to extend that the experimental observations extend to a wider variety of object shapes and roughnesses. Second, additional sensing can be added, such as in the proximal phalange. Third, a new gripper design can be explored, such as including four motors for independent control of each phalange, which would allow for a design that better utilizes the sensor data. Another design change would be to utilize ceramic materials.

VIII. CONCLUSIONS

We present a novel multi-axis tactile sensor for space that is made using a single fiber, allowing for a more compact form factor than previous designs. Optical fibers are particularly advantageous in space applications because of robustness against radiation, EMI, and extreme temperatures. Our initial use case is for Astrobee on the ISS, but can be extended to include EVA as well. We report on early experiments showing how it works in a gripper. we can use the sensor to tell if solid grip and adjust or realign.

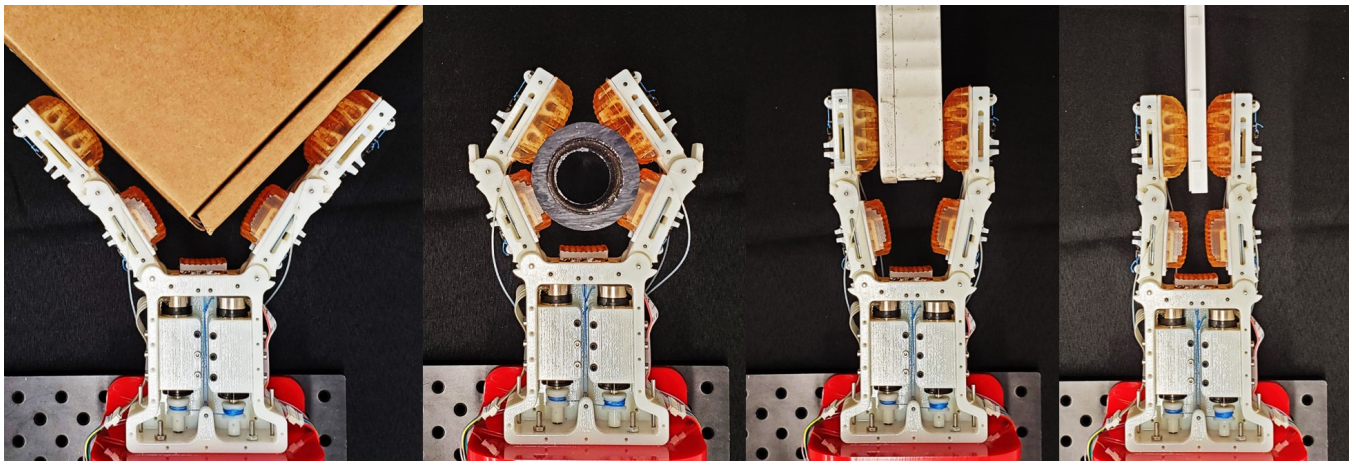

Fig. 6. Grasping different objects...

ACKNOWLEDGMENT

The authors thank the National Aeronautics and Space Administration (NASA) for financial support for this research through the grant from SBIR contract to IFOS and subcontract to Stanford's Center for Design Research. J. Di is additionally supported by a NASA Space Technology Research Fellowship.

REFERENCES

[1] I.-W. Park, T. Smith, H. Sanchez, S. W. Wong, P. Piacenza, and M. Ciocarlie, "Developing a 3-dof compliant perching arm for a free-flying robot on the international space station," in *2017 IEEE International Conference on Advanced Intelligent Mechatronics (AIM)*. IEEE, 2017, pp. 1135–1141.

[2] A. Yamaguchi and C. G. Atkeson, "Recent progress in tactile sensing and sensors for robotic manipulation: can we turn tactile sensing into vision?" *Advanced Robotics*, vol. 33, no. 14, pp. 661–673, 2019.

[3] X. Qiao, Z. Shao, W. Bao, and Q. Rong, "Fiber bragg grating sensors for the oil industry," *Sensors*, vol. 17, no. 3, p. 429, 2017.

[4] S. Park, T. Park, and K. Han, "Real-time monitoring of composite wind turbine blades using fiber bragg grating sensors," *Advanced Composite Materials*, vol. 20, no. 1, pp. 39–51, 2011.

[5] D. L. Presti, C. Massaroni, C. S. J. Leitão, M. D. F. Domingues, M. Sypabekova, D. Barrera, I. Floris, L. Massari, C. M. Oddo, S. Sales, *et al.*, "Fiber bragg gratings for medical applications and future

challenges: A review," *IEEE Access*, vol. 8, pp. 156 863–156 888, 2020.

[6] J.-S. Heo, J.-H. Chung, and J.-J. Lee, "Tactile sensor arrays using fiber bragg grating sensors," *Sensors and Actuators A: Physical*, vol. 126, no. 2, pp. 312–327, 2006.

[7] J.-S. Heo, J.-Y. Kim, and J.-J. Lee, "Tactile sensors using the distributed optical fiber sensors," in *2008 3rd International Conference on Sensing Technology*. IEEE, 2008, pp. 486–490.

[8] J. Song, Q. Jiang, Y. Huang, Y. Li, Y. Jia, X. Rong, R. Song, and H. Liu, "Research on pressure tactile sensing technology based on fiber bragg grating array," *Photonic Sensors*, vol. 5, no. 3, pp. 263–272, 2015.

[9] T. Li, C. Shi, and H. Ren, "A high-sensitivity tactile sensor array based on fiber bragg grating sensing for tissue palpation in minimally invasive surgery," *IEEE/ASME Transactions on Mechatronics*, vol. 23, no. 5, pp. 2306–2315, 2018.

[10] Q. Jiang and L. Xiang, "Design and experimental research on small-structures of tactile sensor array unit based on fiber bragg grating," *IEEE Sensors Journal*, vol. 17, no. 7, pp. 2048–2054, 2017.

[11] S. Samuel, A. Kumar, and C. K. Mukhopadhyay, "Fiber bragg grating tactile sensor for imaging," *Optik*, vol. 198, p. 163062, 2019.

[12] L. Massari, E. Schena, C. Massaroni, P. Saccomandi, A. Menciassi, E. Sinibaldi, and C. M. Oddo, "A machine-learning-based approach to solve both contact location and force in soft material tactile sensors," *Soft robotics*, vol. 7, no. 4, pp. 409–420, 2020.

[13] S. Hu, H. Wang, Y. Wang, and Z. Liu, "Design of a novel six-axis wrist force sensor," *Sensors*, vol. 18, no. 9, p. 3120, 2018.

[14] L. Xiong, Y. Guo, G. Jiang, X. Zhou, L. Jiang, and H. Liu, "Six-dimensional force/torque sensor based on fiber bragg gratings with low coupling," *IEEE Transactions on Industrial Electronics*, 2020.

[15] Y.-L. Park, S. C. Ryu, R. J. Black, K. K. Chau, B. Moslehi, and M. R. Cutkosky, "Exoskeletal force-sensing end-effectors with embedded optical fiber-bragg-grating sensors," *IEEE Transactions on Robotics*, vol. 25, no. 6, pp. 1319–1331, 2009.

[16] L. Massari, C. M. Oddo, E. Sinibaldi, R. Detry, J. Bowkett, and K. C. Carpenter, "Tactile sensing and control of robotic manipulator integrating fiber bragg grating strain-sensor," *Frontiers in neurorobotics*, vol. 13, p. 8, 2019.

[17] L. Jiang, K. Low, J. Costa, R. J. Black, and Y.-L. Park, "Fiber optically sensorized multi-fingered robotic hand," in *2015 IEEE/RSJ International Conference on Intelligent Robots and Systems (IROS)*. IEEE, 2015, pp. 1763–1768.

[18] M. Ciocarlie, F. M. Hicks, R. Holmberg, J. Hawke, M. Schlicht, J. Gee, S. Stanford, and R. Bahadur, "The velo gripper: A versatile single-actuator design for enveloping, parallel and fingertip grasps," *The International Journal of Robotics Research*, vol. 33, no. 5, pp. 753–767, 2014.